

M atching of soft and hard P om erons

Sergey Bondarenko ¹, Eugene Levin ¹ and C-I Tan ²¹ HEP D epartm ent, School of Physics and A stronomy
TelA viv U niversity, TelA viv 69978, Israel² Physics D epartm ent, B rown U niversity,
P rovidence RI 02912, U SA

In this paper an attempt is made to match perturbative BFKL Pomeron with non-perturbative Pomeron originating from non-perturbative QCD phenomena such as QCD instantons and/or scale anomaly. The main idea centers on the fact that the non-perturbative Pomeron involves a large scale ($M_0 \approx 2 \text{ GeV}$), which is larger than the scale starting from which we can use perturbative QCD. One key result is that even for processes involving large hard scale (such as DIS) the low x behavior is determined by an effective Pomeron with an intercept having an essential non-perturbative QCD contribution.

I. IN T R O D U C T I O N

In this paper we present an attempt to solve one of the most challenging problems of QCD: the interface between long distance (non-perturbative, soft) interaction and the short distance one (perturbative, hard) at high energy. The short distance interaction at high energy is controlled by perturbative QCD and can be described by the BFKL equation [1]. We call the hard Pomeron a solution to this equation, in spite of the fact that this solution is not a Regge pole. The region of long distances we describe by introducing the phenomenological soft Pomeron – a Regge pole with the intercept close to 1 [2]. Recently, progress has been achieved in a theoretical understanding of the structure of the soft Pomeron [3{9], which provides hope for developing a first approach to understand the matching of these two Pomerons: the soft Pomeron and the BFKL one.

This hope is based on a new hierarchy of the scales in QCD suggested in Ref. [3] and depicted in Fig. 1.

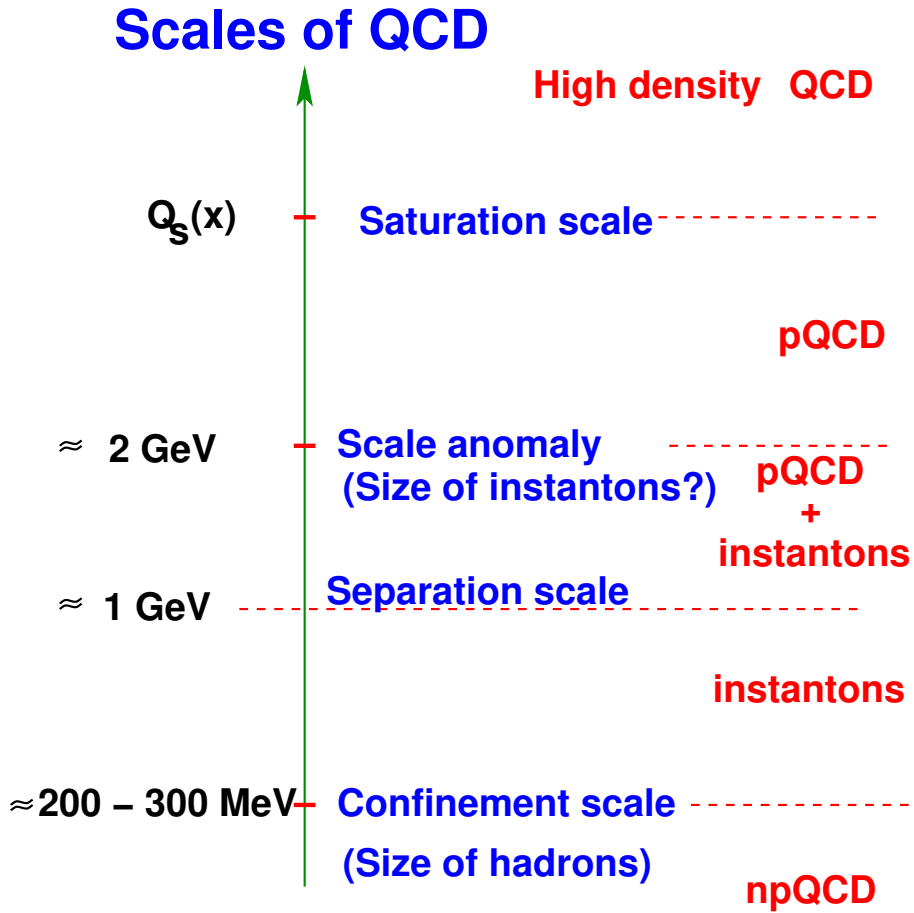


FIG . 1. Scales of QCD accordingly to Ref. [3].

The key idea of this picture is the large scale for the soft Pomeron ($q_s = M_0 \approx 2 \text{ GeV}$) which is closely related to the violation of the scale anomaly of QCD. The value of M_0 is so large that the coupling QCD constant $\alpha_s(M_0) \ll 1$ and it can be considered as a small parameter. As one can see in Fig. 1 such a sequence of scales makes possible a theoretical approach to the problem of matching of soft and hard Pomerons. Indeed, for all virtualities (transverse momenta) larger than the separation scale, $q > q_H \approx 1 \text{ GeV}$, where $\alpha_s(q^2) < 1$, we can apply the perturbative QCD approach.

We, therefore, formulate the problem of the interface between soft and hard Pomeron as a problem of matching the perturbative BFKL Pomeron with the soft Pomeron based on the non-perturbative contributions with sufficiently high scale (see Fig. 1). Of course, a lot of non-perturbative contributions originate from very long distances of the order of the confinement scale (see Fig. 1) but we assume that all of them are irrelevant to the structure of the soft Pomeron [3].

We also assume that the energies are so high that the saturation scale [10,11] is much larger than the scale anomaly scale, (or scale of the soft Pomeron), $q_s \approx M_0 \approx 2 \text{ GeV}$ and the separation scale q_H which characterizes that value of the virtuality (transverse momentum) from which we can start using perturbative QCD. Our notation is transparent since q_s gives the scale of the soft Pomeron while for $q > q_H$ we can use the BFKL Pomeron to describe the high energy scattering in pQCD.

In the next section we describe the general formalism of our approach which leads to a new Regge pole as a result of matching between soft and hard Pomerons with the trajectory $\alpha_{sH}(t) = 1 + \alpha_{sH} + \frac{0}{s_H} t$. Section 3 is devoted entirely to the properties of the Green function of the BFKL Pomeron with the running QCD coupling constant. As it has been shown in many papers [10,12{18}] the QCD running coupling changes the character of the singularity in the BFKL Pomeron which becomes an essential singularity at $! = 0$ instead of the pole at $! = !_L$. In this section we present a detailed analysis of the Green function for the BFKL equation which is similar to the paper [18] which appeared after we had finished our calculations.

In section 4 we calculate the trajectory of the soft Pomeron which leads to the phenomenological Pomeron ($\alpha_{\text{phenom } P} = 1 + 0.08 + 0.25 \text{ GeV}^{-2} t$) and which appears as a result of matching of the BFKL and soft Pomérons in our approach. The deep inelastic scattering in the region of rather low virtualities of photon is discussed in section 5 where the values of virtualities for the hard processes are specified using our approach for matching.

II. GENERAL APPROACH

In this section we will outline the general approach for the matching of soft and hard Pomérons. To do this we need to specify our description of the soft Pomeron based on general ideas of Ref. [3]. We next review the key feature of BFKL Pomeron in the LLA, elaborate its Green's function in the Airy model, and finally discuss unifying soft and hard Pomérons.

A. Soft Pomeron

As a working model for the soft Pomeron we shall adopt the QCD instanton approach [4]. This is in fact not necessary since we only need to use general properties of the soft Pomeron exchange depicted in Fig. 2.

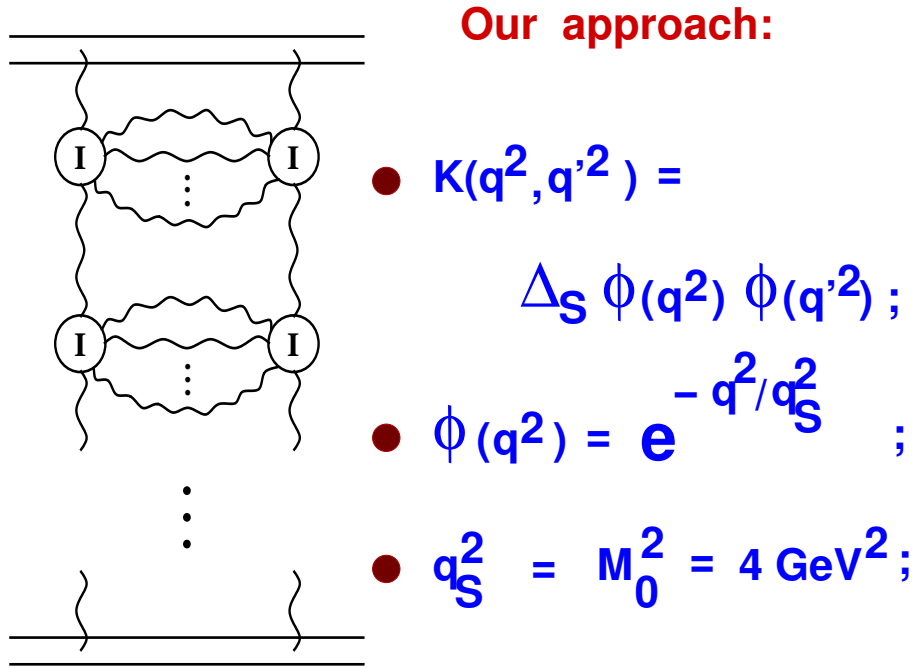


FIG. 2. The main properties of the soft Pomeron originated from the QCD instanton approach [4]

As shown in Ref. [4], the structure of the soft Pomeron in the instanton approach formally reduces to summing the ladder diagrams of Fig. 2. These ladder diagrams describe the t-channel gluon that propagates through the space inducing a chain of instanton transitions between different vacua and producing a number of gluons in each transition. The sum of these diagrams leads to power-like (Regge-type) asymptotic, namely the scattering amplitude $A(s; t)$ is asymptotically equal to

$$A(s; t) = g(t) s^{\alpha_P(t)}; \quad (1)$$

with $\alpha_P(t) = 1 + \alpha_S + \frac{0}{S} t$. It is well known (see Ref. [19]) that both α_S and $\frac{0}{S}$ can be found as solutions of the Bethe-Salpeter type equation resulting from these ladder graphs. In this paper, we shall

concentrate on the forward scattering limit, $t = 0$, where the kernel $K(q^2; q'^2)$ is a function of transverse momenta, q and q' , along adjacent rungs of the ladder in Fig. 2. We assume that this kernel has the general factorized properties, namely $K(q^2; q'^2) = \frac{1}{s} K(q^2) K(q'^2)$ which follow from the instanton approach of Ref. [4] but could have a more general validity.

B. BFKL Pomeron

The BFKL Pomeron gives the high energy asymptotic for the scattering amplitude in the so-called leading $\log(1/x)$ approximation (LLA) of perturbative QCD [1]. In the LLA, for each set of Feynman diagrams of the order of $\frac{1}{s}$, one keeps only leading terms proportional to $(\alpha_s \ln(1/x))^n$, and sum over these terms. It turns out that in LLA this sum also formally reduces to a summation of "gluon ladder" diagrams, (see Fig. 3).

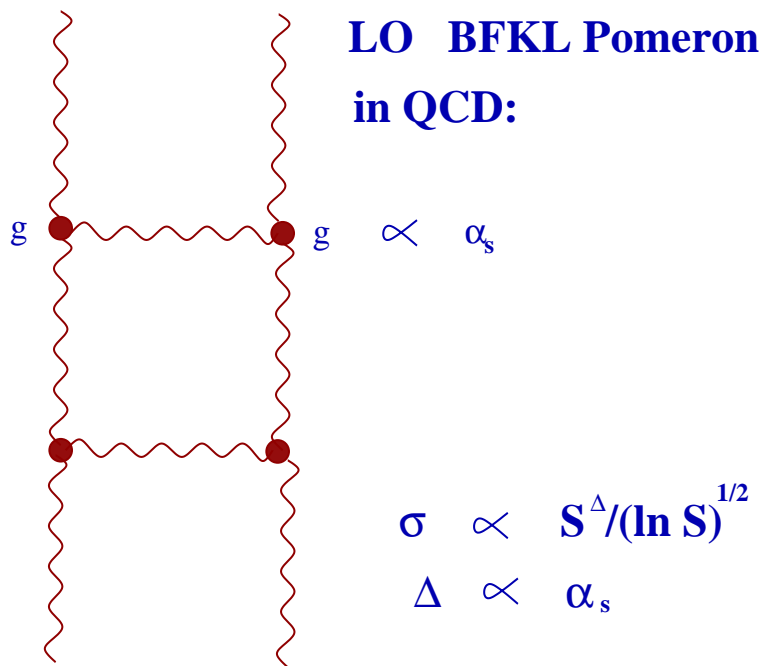


FIG. 3. The BFKL Pomeron in LLA.

However, due to the specific property of the vertex [1], the sum of these "ladder" diagrams leads to an amplitude $A(s;t) / s^H = \frac{1}{\ln(s)}$, with $H = \frac{1}{s}$. The presence of the additional $1 = \ln(s)$ factor reflects the fact that the BFKL Pomeron is actually not a Regge pole.

For further discussion, it is more convenient to work in the complex angular momentum plane, $l = 1 + !$, and to restrict ourselves to the forward limit $t = 0$. In particular, we need to find the Green function¹ $G_! (q_f; q_l)$ for the BFKL equation which satisfies the following equation (see Refs. [15,16,18] for details and Fig. 4 for graphical form of the equation)

$$! G_! (q_f; q_l) = \int \frac{d^2 q^0}{(2\pi)^2} K(q_f; q^0) G_! (q^0; q_l) : \quad (2)$$

¹We shall also denote this Green function as $G_!^H$ to emphasize that it is responsible for the "hard" perturbative QCD contribution.

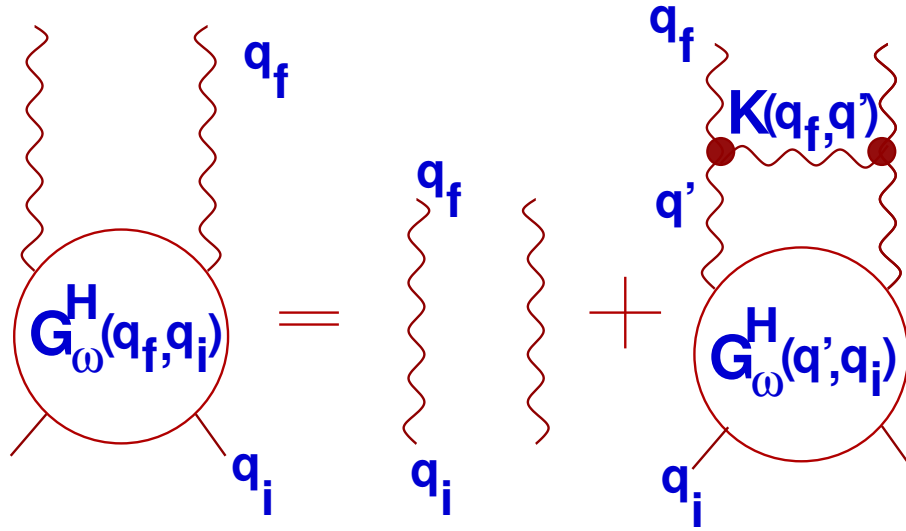


FIG. 4. The BFKL equation for the Green function

The kernel $K(q_f; q')$ in Eq. (2) can be written, after integration over the azimuthal angle, in the form

$$K(q_f; q') = \int_s(q_f^2) K \frac{q_f^2}{q'^2} ; \quad (3)$$

It can be shown that functions

$$f_s(q^2) = \int_s \frac{q^2}{(q^2)^s} ; \quad (4)$$

satisfy a generalized eigenvalue equation

$$\int_s(q^2) \int_{dq'^2} K \frac{q'^2}{q'^2} f_s(q'^2) = \frac{r_H}{r} \int(f) f_s(q^2) ; \quad (5)$$

with $\int(f)$ as eigenvalues. Here, $r = \ln(q^2 = \mu^2) - \frac{1}{2} \ln \int_s(q^2)$, $r_H = \ln(q_H^2 = \mu^2)$, and $\int(f)$ in leading order of pQCD is equal to

$$\int(f) = -\frac{s(r_H)}{s} N_c \int_0^1 \left(\frac{1}{2} - f \right) \left(\frac{1}{2} + f \right) g ; \quad (6)$$

In this paper we mostly use the expansion of $\int(f)$ at small values of f , namely,

$$\int(f) = \int_L - 1 + D f^2 + O(f^4) ; \quad (7)$$

It should also be stressed that in Eq. (6) and Eq. (7) the normalization point for the QCD running coupling constant \int_s was chosen as the separation scale, namely $\int_s(q_H^2)$.

The solution to the inhomogeneous Eq. (2) can be found by expanding $G!(r_f; r_i)$ in terms of the complete set of eigenfunctions, Eq. (4),

$$G!(q_f; q_i) = G!(r_f; r_i) = \int_{a-i1}^{a+i1} \frac{df}{2-i} g(!; f; r_i) \int_s(q^2) = \int_{a-i1}^{a+i1} \frac{df}{2-i} g(!; f; r_i) e^{rf} ; \quad (8)$$

$$G(Y; r_f; r_i) = \frac{1}{q_f q_i} \int \frac{d!}{2-i} e^{!Y} G!(r_f; r_i) ; \quad (9)$$

where $Y = \ln(s=q_f q_i)$.

Using Eq. (8) one obtains the following equation for $g(!;f;r_i)$ [16]

$$! \frac{dg(!;f;r_i)}{df} = r_H ! (f) g(!;f;r_i) + r_i e^{f r_i} : \quad (10)$$

As a first order differential equation, Eq. (10) can be solved analytically. The solution to Eq. (10) can be written as the sum of two terms, [16]:

$$g_1(!;f;r_i) = \frac{r_i}{2!} \int_f^Z df^0 e^{f^0 r_i + \frac{r_H}{!} R_{f^0} ! (f^0) df^0} ; \quad (11)$$

and

$$g_2(!;f;r_i) = \frac{r_i}{2!} \int_f^Z df^0 e^{f^0 r_i + \frac{r_H}{!} R_{f^0} ! (f^0) df^0} ; \quad (12)$$

where the integration path in Eq. (11) is a ray C_1 , from f to infinity, laying between the polar angles $\theta=3$ and $\theta=2$ and the corresponding path for Eq. (12) is another ray C_2 from f to minus infinity, laying between the polar angles $\theta=3$ and $\theta=2$. That is, for $G(r_f;r_i)$, we obtain

$$G!(r_f;r_i) = \int_{f-i}^{f+i} \frac{df}{2!} e^{f r_f} (g_1(!;f;r_i) + g_2(!;f;r_i)) : \quad (13)$$

It is worthwhile mentioning that the difference between Eq. (11) and Eq. (12) is a solution to the homogeneous BFKL equation with the running QCD coupling constant, (Eq. (10) without the inhomogeneous term). The fact that $g(!;f;r_i) = g_1(!;f;r_i) + g_2(!;f;r_i)$ corresponds to having chosen the integration constant to Eq. (10) in order to assure that $G!(r_f;r_i)$ is real.

C. The BFKL Green function in the Airy model

To clarify the main properties of the Green's function we consider the expansion of Eq. (7) which is justified at small values of f and f^0 . We call this approach the Airy model, as it was first done in Ref. [18], since our functions will be very close to the Airy functions. Using new variables $f^+ = f^0 + f$ and $f^- = f^0 - f$, we can reduce Eq. (13) to the form

$$g(!;r_f;r_i) = \frac{r_i}{4!} \int_{f-i}^{f+i} \frac{df^+}{2!} \int_{C_1}^Z df e^{(!;f^+;f^-;r_f;r_i)} + \int_{C_2}^Z df e^{(!;f^+;f^-;r_f;r_i)} \quad (14)$$

$$(!;f^+;f^-;r_f;r_i) = \frac{r_f + r_i}{2} f^- + \frac{r_f - r_i}{2} f^+ + \frac{! r_H}{!} f^- f^+ + \frac{D}{3} \left[\frac{3}{4} (f^+)^2 + \frac{1}{4} (f^-)^2 \right] g ; \quad (15)$$

Integration paths C_1 and C_2 in Eq. (14) are still defined in the same way as in previous section, with the starting shifted to $f^- = 0$.

Since the f^+ -integral is Gaussian, we have

$$g(!;r_f;r_i) = \frac{r_i}{16!} \frac{r_i^2}{! r_H D} \int_{C_1}^Z \int_{C_2}^Z \frac{df}{f} e^{f \left[\frac{r_f + r_i}{2} f^- + (f^-)^3 \frac{D! r_H}{12!} + \frac{1}{f} \left(\frac{f^-}{2} \right)^2 \frac{!}{! r_H} \right]} ; \quad (16)$$

with the $t = \frac{r_H !}{r_f + r_i}$ and $r = \frac{r_f - r_i}{r_f + r_i}$. We can change variable further to: $f^- = \frac{4!}{D! r_H} f$, and obtain for our Green function:

$$g(!; r_f; r_i) = \frac{s}{16} \frac{r_i^2}{!!_L r_H D} \frac{4!}{!!_L r_H D} \frac{1}{6} \tilde{A}i(;) ; \quad (17)$$

$$\tilde{A}i(;) = \frac{1}{c_1} + \frac{d}{c_2} e^{\frac{1}{3}} + \frac{3}{3} \frac{2}{2} ; \quad (18)$$

$$= \frac{D}{4!} \frac{!!_L r_H}{2} \frac{1}{2} \frac{r_f + r_i}{!!_L r_H} g ; \quad (19)$$

$$= \frac{r}{2} \frac{!!}{2D !!_L r_H} \frac{1}{3} \text{ with } r = r_f - r_i ; \quad (20)$$

Once $g(!; r_f; r_i)$ is known, the asymptotic behavior of our Green function $G(Y; r_f; r_i)$ can be obtained from Eq. (9). However, in dealing with the general expression (see Eq. (17)–Eq. (20)) we have to take into account that the limit depends on the virtualities r_f and r_i , in particular, the value $\frac{1}{2}$. Further, ultimately, we need also to take into account the soft Pomeron intercept. For different relations between these two values, different regions in the $!$ integral can dominate, leading to different asymptotic behavior for the Green function. We start the search for the resulting singularities by considering various situations where different regions of $!$ dominating the integral in Eq. (9).

Let us first consider the case when $! \gg \frac{1}{2}$. In this region both (Eq. (19)) and (Eq. (20)) are large, and therefore we can hope that the main contribution in this integral comes from the region of small $!$. Neglecting the $e^{-\frac{1}{3}}$ term in the exponent of the integrand, we obtain

$$\tilde{A}i(;) / \int_0^{\frac{1}{2}} \frac{d!}{!} e^{-\frac{1}{3}} \quad (21)$$

We will see later, that omitted $e^{-\frac{1}{3}}$ term is indeed small. For such integral the integration over two different contours in Eq. (13) give the same answer, since the integrand has no singularities in the right semiplane and both integrals could be taken along the real axis. The resulting integral can be evaluated explicitly, leading to:

$$\tilde{A}i(r_i; r_f) / 2K_{\frac{1}{2}}(r) \frac{r}{!!_L r_H D} \frac{1}{\frac{1}{2}} \frac{1}{1-2} \quad (22)$$

where $K_{\frac{1}{2}}(z)$ is the modified (Macdonald) Bessel function. Since Eq. (21) does not depend on the sign of r , therefore we can write the answer as

$$g(!; r_f; r_i) = G_{\frac{1}{2}}^{\frac{1}{2}}(r_f; r_i) = \frac{r_i}{2r^{1-2}} \frac{1}{!!_L r_H D} e^{2(\frac{r}{2})^{\frac{1}{2}}} P_{\frac{1}{2}}^{\frac{1}{2}}(\frac{r}{D}) (r) + e^{2(\frac{r}{2})^{\frac{1}{2}}} P_{\frac{1}{2}}^{\frac{1}{2}}(\frac{r}{D}) (r) ; \quad (23)$$

If we will integrate over r , we could simply integrate over the following function but only for positive values of r :

$$G_{\frac{1}{2}}^{\frac{1}{2}}(r_f; r_i) = \frac{r_i}{r^{1-2}} \frac{1}{!!_L r_H D} e^{2(\frac{r}{2})^{\frac{1}{2}}} P_{\frac{1}{2}}^{\frac{1}{2}}(\frac{r}{D}) ; \quad (24)$$

where $r = \frac{r_i + r_f}{2} \frac{!!_L r_H}{!}$. One can see that, in this region, r and r_i are small, $r \frac{1}{!!_L r_H} \ll 1$ and $\frac{1}{32!} \frac{1}{32!} \ll 1$. Therefore we can trust this solution so long that the following condition is satisfied:

$$\frac{1}{!!} \ll 1 ; \quad (25)$$

Indeed, even when $\frac{1}{!!} = 1$, the $\frac{1}{32!}$ is still small, $\frac{1}{32!} \ll 1$: The magnitude of omitted term in our solution is also small, namely, $e^{\frac{1}{32!} \frac{1}{(\frac{r_i + r_f}{2})^2}}$, and we have more exactly for the Green function in this region:

$$G^1(x^0; x^0) = \frac{r^0}{x^{1=2}} \frac{r}{!!_L r_H D} e^{r \frac{p}{D \frac{1}{t}} + \frac{1}{96} \frac{p}{!!_L \frac{1}{(x^0 + x^0)^2}}}; \quad (26)$$

This equation gives the asymptotic answer of Green's function for the case $! \gg t$ in so called diffusion approximation for the BFKL kernel.

Let us now consider the integral over $!$ with the contour of integration in Eq. (26) defined in a usual way: to the right of all singularities of the integrand. First consider the limit $Y \rightarrow 0$:

$$G^1(0; r_f; r_i) = \frac{2 r_i}{r_i + r_f} \frac{r}{t D} \int_{t-i1}^{t+i1} \frac{d!}{2-i} e^{r \frac{p}{D \frac{1}{t}}} : \quad (27)$$

Closing the contour of integration to the left over the cut from the 1 to t with the variables change:

$$! = t - e^i ! \quad (28)$$

on the upper edge of the cut, and

$$! = t - e^i ! \quad (29)$$

on the lower edge of the cut. In so doing, the integral Eq. (27) turns into a sum:

$$G^1(0; r_f; r_i) = \frac{2 r_i}{r_i + r_f} \frac{r}{t D} \int_0^1 \frac{d!}{2-i} e^{i r \frac{p}{D \frac{1}{t}}} + \frac{2 r_i}{r_i + r_f} \frac{r}{t D} \int_1^0 \frac{d!}{2-i} e^{i r \frac{p}{D \frac{1}{t}}}; \quad (30)$$

or

$$G^1(0; r_f; r_i) = \frac{2 r_i}{r_i + r_f} \int_0^1 \frac{d!}{2} e^{i r !} + \frac{2 r_i}{r_i + r_f} \int_1^0 \frac{d!}{2} e^{i r !}; \quad (31)$$

which leads to (after changing variable $!!$ in the second term of this expression)

$$G^1(0; r_f; r_i) = \frac{2 r_i}{r_i + r_f} \int_1^1 \frac{d!}{2} e^{i r !} = \frac{2 r_i}{r_i + r_f} {}^{(2)}(r); \quad (32)$$

Coming back to Eq. (27) with non zero Y , we have

$$G^1(r_f; r_i) = \frac{2 r_i}{r_i + r_f} \frac{r}{t D} \int_{t-i1}^{t+i1} \frac{d!}{2-i} e^{! Y} e^{r \frac{p}{D \frac{1}{t}}}; \quad (33)$$

This integral can be evaluated using the steepest descent method, with the saddle point in $!$ determined by:

$$Y - \frac{r}{2} \frac{1}{D \frac{1}{t}} \frac{1}{!!} = 0; \quad (34)$$

In the limit $! \gg t$, Eq. (34) leads to the following saddle point value:

$$!_{SP} = \frac{r}{2} \frac{1}{Y^2} \frac{1}{t D}; \quad (35)$$

and to the asymptotic behavior of the Green function:

$$G^1(Y; r_f; r_i) = \frac{r}{2} \frac{1}{Y t D} e^{-\frac{(r)^2}{4 Y t D}}; \quad (36)$$

which is valid for $!_{SP} \gg t$, or $! = Y \gg t$, or $Y \ll \frac{1}{t}$.

There is another contribution in the limit of $! \gg t$ coming from the large $!$ region. Indeed, it is easy to see from Eq. (18), that there is another saddle point,

$$f_{SP}^2 \approx 0: \quad (37)$$

In the region $\omega \gg 1$ we have

$$f_{SP} = \sqrt{p} = \frac{1}{r_f} \frac{p}{\sqrt{1}} \quad (r_H, D=4) \frac{1}{\omega} \gg 1: \quad (38)$$

This saddle point corresponds to the second crossing point of Fig. 5. This is solution for the for $\omega \gg 1$.

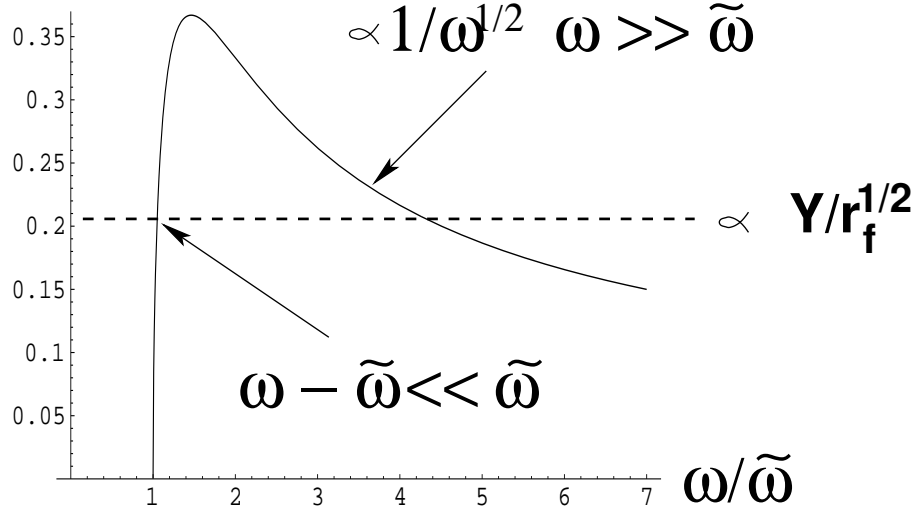


FIG. 5. The positions of the saddle points in ω for $G(y; r_f; f_f)$ for $\omega \gg 1$.

However, it turns out that in this regime, $f_{SP} \approx 1$ while f_{SP}^+ is small ($f_{SP}^+ \approx 1$). It follows that we can not use diffusion approach for the BFKL equation for an estimate of this contribution. In this case Eq. (17)-Eq. (18) are no longer valid, and we have to take the full kernel of Eq. (6) into consideration. The integration over this full kernel is performed along the real axis and instead of two solutions Eq. (11) and Eq. (12) now we have only one. Going back to variables f^+ and f^- and considering $f^+ = f^- \ll 1$, one can obtain the following equation for the saddle point:

$$r_f \frac{2 r_H}{\omega} \frac{s(r_H) N_c}{1} \frac{1}{f_{SP}} = 0 \quad (39)$$

Eq. (39) stems from the fact that in the region of large ω , f^- is rather large. For large f^- we can replace $\omega(f^-)$ by $\omega(f^-) \approx \frac{s(r_H) N_c}{1} \frac{2}{f_{SP}}$. Thus we have

$$1 - f_{SP} = \frac{2\omega}{\omega} = 1: \quad (40)$$

We obtain for the Green function in this region of ω :

$$G_{\omega}^2(r_i; r_f) \approx \frac{p}{\omega} e^{\frac{r_i + r_f}{2} - \frac{2 s(r_H) N_c r_H}{\omega} \ln\left(\frac{\omega}{\omega}\right)} \quad (41)$$

For the ω -saddle point, we have

$$Y + \frac{2 s(r_H) N_c r_H}{\omega_{SP}^2} \ln\left(\frac{\omega}{\omega_{SP}}\right) = 0; \quad (42)$$

which leads to

$$\omega_{SP} = \frac{2 s(r_H) N_c r_H}{Y} \ln \frac{2 s(r_H) N_c r_H}{Y \omega_{SP}^2} \quad (43)$$

Using Eq. (43), we arrive at

$$G(Y; r_f; r_f) \approx e^{\frac{q}{2} \frac{2 s(r_H) N c r_H}{Y} \ln \frac{2 s(r_H) N c r_H}{Y t^2}} ; \quad (44)$$

This contribution has been missed in Refs. [16,18]. Nevertheless, comparing Green functions of Eq. (26) and Eq. (41), we see, in the limit of small t , the contribution of Eq. (26) is larger, than the contribution of Eq. (41):

$$\frac{G_1^2(r_i; r_f)}{G_1^1(r_i; r_f)} \approx e^{\frac{r_i + r_f}{2}} ; \quad (45)$$

We next consider the limit where l is close to t : $l = t + \delta$, i.e., $l = t \ll 1$. In this case l is small, $\delta \ll 1$, indeed, $\frac{l-t}{l} / \frac{1}{t} \ll 1$, and for small l we have $l \approx t$. We also take r in the limit $r \ll (4\pi D)^{1/3}$ and, therefore, we neglect the $l^2 =$ term in our equation. Now we need to consider both solutions of Eq. (10) together, sum of Eq. (11) and Eq. (12). Due to the integration along the rays $\theta = 3$ and $\theta = 3$ we have:

$$g(l; r_f; r_f) / e^{i=6} \approx \int_0^1 \frac{d\theta}{\theta} e^{-e^{i=3} \frac{3}{\theta}} + e^{i=6} \int_0^1 \frac{d\theta}{\theta} e^{-e^{i=3} \frac{3}{\theta}} ; \quad (46)$$

These functions are complex conjugated and, therefore, the answer is the sum of the real parts of these functions:

$$g(l; r_f; r_f) / 2 \cos(\theta=6) \approx \int_0^1 \frac{d\theta}{\theta} e^{-\cos(\theta=3) \frac{3}{\theta}} \cos(\theta \sin \frac{\theta}{3}) + 2 \sin(\theta=6) \int_0^1 \frac{d\theta}{\theta} e^{-\cos(\theta=3) \frac{3}{\theta}} \sin(\theta \sin \frac{\theta}{3}) ; \quad (47)$$

Because θ and l are small, while l is the order of 1, we can expand our function with respect to θ -term. Integrating this expansion over θ we obtain the following result for the first two orders of θ :

$$g(l; r_f; r_f) / \frac{(\frac{1}{6})}{3^{2=3}} \approx 2 \frac{(\frac{5}{6})}{8 \cdot 3^{4=3}} ; \quad (48)$$

Taking into account expression for l :

$$= \frac{4!}{D!_L r_H} \frac{1=3}{2} \frac{r_i + r_f}{l} (l \approx t) ;$$

we obtain finally:

$$g(l; r_f; r_f) / \frac{(\frac{1}{6})}{3^{2=3}} \approx \frac{4!}{D!_L r_H} \frac{2=3}{8!^2} \left(\frac{5}{6}\right)^2 \frac{(\frac{5}{6})}{3^{4=3}} ; \quad (49)$$

This answer is also valid for the case when $l \approx t = 1$ and $l = 1$. In this case, the series of Eq. (48) will be convergent due the $\frac{1}{n!}$ in e expansion. Indeed, we see from Eq. (48), taking $l = 1$, that

$$\frac{(\frac{5}{6})}{(\frac{1}{6}) 8 \cdot 3^{2=3}} / \frac{1}{80} \ll 1 ;$$

is small. The following condition for l arises in this case: $l \approx 3$, and we obtain the simple estimate for the region of l where the series is still convergent and the given solution is still valid:

$$\frac{l}{t} \approx 3 ; \quad (50)$$

where we still have $\frac{1}{\tau} \ll 2$: Now, if we go back to the Eq. (26), and take even $\tau = \tau_0$, we see, that the correcting term to Eq. (26) is still small,

$$e^{-\frac{D \tau_0}{2(r_0+r_1)^2}} \ll 1 + \frac{1}{96} \ll 1$$

Therefore, in the case $\tau = \tau_0$ and $\tau_0 \ll 1$ we obtained overlapping solutions for Green function, Eq. (26) and Eq. (48), which match each other. This completes our consideration, and we now know the form of our Green function in the whole region of positive τ .

We also can find our $G(Y; r_f; r_i)$ function. Indeed, integrating Eq. (47) over τ in the first approximation in τ we have:

$$G(Y; r_f; r_i) / \int_{i_1}^{Z_1} \frac{d(\tau)}{2 \tau} e^{\tau Y + Y \tau} \approx \frac{4}{D \tau_L \tau_H} \int_{i_1}^{Z_1} \frac{r_1 + r_f}{2 \tau^{2=3}} \cos(\tau=3) \tau \approx e^{-\frac{3}{3}}; \quad (51)$$

or

$$G(Y; r_f; r_i) / e^{\tau Y} \int_1^{Z_1} \frac{d(\tau)}{2} e^{i \tau Y} \approx \frac{4}{D \tau_L \tau_H} \int_1^{Z_1} \frac{r_1 + r_f}{2 \tau^{2=3}} \cos(\tau=3) \tau \approx e^{-\frac{3}{3}}; \quad (52)$$

or

$$G(Y; r_f; r_i) / e^{\tau Y} \int_0^{Z_1} \tau \approx \left(Y \frac{4}{D \tau_L \tau_H} \int_0^{Z_1} \frac{r_1 + r_f}{2 \tau^{2=3}} \cos(\tau=3) \tau \right) e^{-\frac{3}{3}}; \quad (53)$$

The final answer, obtained for this Green function in this asymptotic limit, is:

$$G(Y; r_f; r_i) = \frac{r}{8 Y \tau_L \tau_H D} e^{\tau Y} \frac{3 r_i}{9 \tau^{2=3}} \frac{D (\tau Y)^3}{(r_f + r_i)^{2=4}} \quad (54)$$

The region of applicability of this saddle point analysis stems from condition that f^+ and f should be small in order to use the expansion of Eq. (7) and from $\tau_{SP} < \tau$. It is easy to see that these conditions restrict the value of rapidity Y [13,16,18]

$$0 < Y < \frac{r_f^2}{\tau_L \tau_H}; \quad (55)$$

Now, if we consider together the asymptotic behavior of the Green function given by Eq. (36) and Eq. (54), we see that in large range of rapidity, given by Eq. (55), the contribution of Eq. (54) is much larger than contribution Eq. (36). We see, therefore, that the main contribution to the Green's function gives the region of such τ , where $\tau < \tau_0$.

In the region of small $\tau < \tau_0$ where τ is negative (see Eq. (19)), the saddle point of τ is equal to

$$\tau_{SP} = i \frac{\tau_L \tau_H}{D} \frac{1}{3}; \quad (56)$$

Performing calculations for the saddle point we arrive at

$$\tau_{SP} = (1 - i) \frac{r}{D 3 Y}; \quad (57)$$

The Green function is [18]

$$G(Y; r_f; r_i) \approx e^{\frac{r}{3D} \frac{\tau_L \tau_H Y}{3}} \cos \frac{r}{3D} \frac{\tau_L \tau_H Y}{3}; \quad (58)$$

It turns out that restrictions $f_{SP}^+ < 1$ and $f_{SP} < 1$ can be satisfied but only within numerical accuracy, namely, $f_{SP} < 1 = D$. We will see later that D is rather large.

D . Soft to BFK L P o m e r o n t r a n s i t i o n

The main idea of the paper is shown in Fig. 6. Since both scales: soft Pomeron and separation scales, are large we can rewrite the sum of the diagrams in Fig. 6 in the following symbolic way

$$S + SHS + SHSHS + \dots = \frac{S}{1 + HS} \quad (59)$$

Therefore, for the resulting contribution we have the equation, using the properties of the soft Pomeron shown in Fig. 2,

$$G_{\text{I}}^{S \text{ H}}(r_f; r_i) = \frac{R}{1 - s} \int_{r^0}^{r^S} \int_{r^0}^{r^S} (r^0) G_{\text{I}}^{\text{H}}(r^0; r^0) (r^0) ; \quad (60)$$

where G_{I}^{H} is the Green function discussed in the previous subsection.

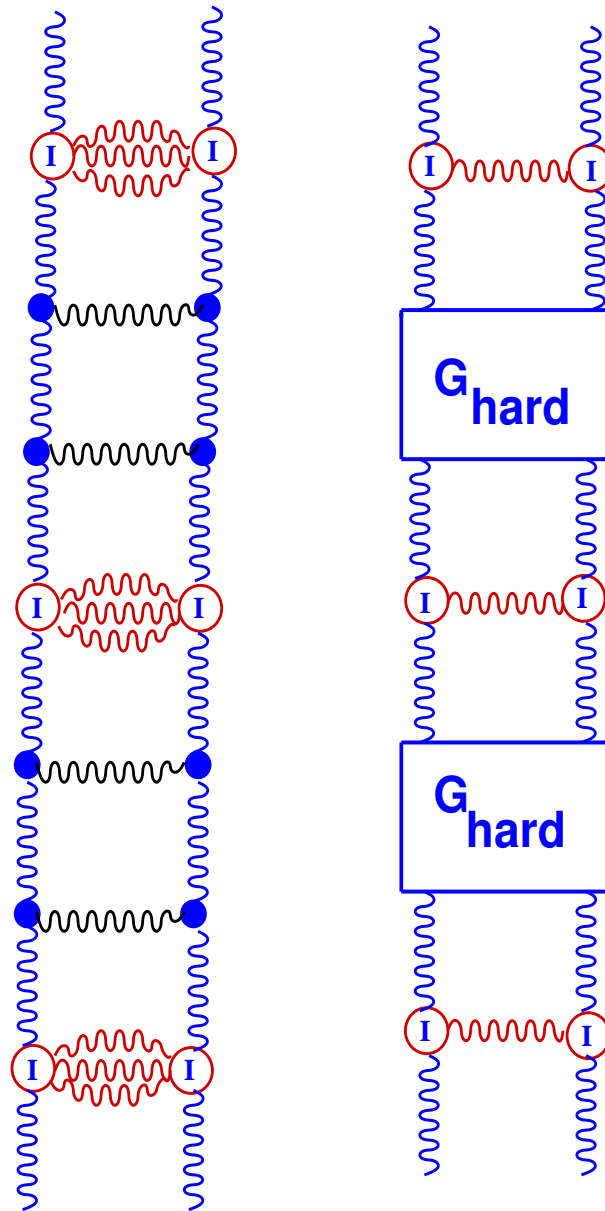


FIG . 6 . D i a g r a m s a n d g r a p h i c f o r m o f e q u a t i o n f o r s o f t t o B F K L P o m e r o n t r a n s i t i o n .

Eq. (60) has poles which are the zeros of the denominator, namely,

$$1 - \int_s^Z \frac{Z}{dr^0} - \int_{dr^0}^Z \frac{Z}{dr^0} (r^0) G_{\frac{1}{2}}^H(r^0; r^0) (r^0) = 0 : \quad (61)$$

To calculate the $G_{\frac{1}{2}}^H(r^0; r^0)$ in this equation, we use the result of Eq. (26) and Eq. (49) for different regions of $! .$ For $! \gg \frac{1}{2}$ we can use the following asymptotic expression:

$$G_{\frac{1}{2}}^H(r^0; r^0) = \frac{r^0}{r^{1=2}} \frac{r}{! ! L r_H D} e^{-r} P_{\frac{1}{D \frac{1}{2}} + \frac{1}{96} \frac{D \frac{1}{2}}{(r^0 + r^0)^2}} ; \quad (62)$$

while for $! \ll \frac{1}{2}$, $\frac{1}{!} \ll 1$, as well as for $! ; \frac{1}{!} \ll 1$ we can use the asymptotic answer for Green function given by Eq. (49):

$$G_{\frac{1}{2}}^H(r^0; r^0) = \frac{r^0}{4} \frac{r}{! ! L r_H D} \frac{4 !}{! L r_H D} \frac{1=6}{3^{2=3}} \frac{(\frac{1}{6})}{D ! L r_H} \frac{2=3}{8 !^2} \left(! \right)^2 \frac{(\frac{5}{6})}{3^{4=3}} : \quad (63)$$

Let us now consider Eq. (61) with using Eq. (62) for $G_{\frac{1}{2}}^H(r^0; r^0)$:

$$1 - \int_s^Z \frac{Z}{dr^0} - \int_{dr^0}^Z \frac{Z}{dr^0} (r^0) G_{\frac{1}{2}}^H(r^0; r^0) (r^0) = 0 : \quad (64)$$

Using new variables

$$x = \frac{r^0 + r^0}{2} ; \quad y = \frac{r^0 - r^0}{2} ; \quad (65)$$

in Eq. (64), we obtain:

$$\frac{s}{! \frac{1}{2}} e^{\frac{1}{96} \frac{D \frac{1}{2}}{! r_s^2}} \frac{r}{D \frac{1}{2}} \int_0^Z \frac{Z}{!} dy \int_0^Z \frac{Z}{!} dx e^{-y} P_{\frac{1}{D \frac{1}{2}}} e^{\frac{2}{q_s^2} \cosh(y) e^x} ; \quad (66)$$

In Eq. (66) we have used $\frac{r^0 + r^0}{2} = r_s$ and defined $\frac{1}{2} = \frac{! r_H}{r_s}$.

In the limit of small $! \rightarrow 0$ we have $y / \frac{1}{2} \rightarrow 0$ and, therefore, we can write the integral in the form:

$$\frac{s}{!} e^{\frac{1}{96} \frac{D \frac{1}{2}}{! r_s^2}} \frac{r}{D \frac{1}{2}} \int_0^Z \frac{Z}{!} dy e^{-y} P_{\frac{1}{D \frac{1}{2}}} \int_0^Z \frac{Z}{!} dx e^{\frac{2}{q_s^2} e^x} ; \quad (67)$$

or

$$\frac{s}{!} e^{\frac{1}{96} \frac{D \frac{1}{2}}{! r_s^2}} \int_0^Z \frac{Z}{!} dy e^{-y} \int_0^Z \frac{Z}{!} dx (x)^2 = \frac{s}{!} e^{\frac{1}{24} \frac{D \frac{1}{2}}{! r_s^2}} ; \quad (68)$$

It follows that the equation for the intercept of the resulting pole is:

$$1 - \frac{s}{! \frac{1}{2}} e^{\frac{1}{96} \frac{D \frac{1}{2}}{! r_s^2}} = 0 ; \quad (69)$$

or

$$1 - \frac{s}{! \frac{1}{2}} \left(1 + \frac{D \frac{1}{2}}{96 ! r_s^2} \right) = 0 : \quad (70)$$

This leads to a simple solution:

$$! = s_H = s + \frac{1}{2} + \frac{D \frac{1}{2} s}{96 r_s^2 (s + \frac{1}{2})} ; \quad (71)$$

Therefore, the intercept of the resulting pole is simply $s_H = s$ for $t_s \neq 0$. This result is obvious from the beginning since for $t_s = 0$ there is no perturbative emission of gluons. It should be stressed, that this answer is obtained within the restriction,

$$t_s \gg t; \quad (72)$$

see also Eq. (25).

It is easy to see, that this restriction is satisfied when t_s is small. This happens in two cases:

when s is small. In this case t is also small and, therefore, from Eq. (72) we have:

$$s \gg t_s \quad t; \quad (73)$$

We can perform here the simple numerical estimate: for the $s = 0.1$ we have $t_L = 0.18$ ($t_s = 0.1$) (see next section), so taking $t = s_H = 0.2$ we obtain $s = 0.1$, where $s > t_s = t$. So, one can see that restriction Eq. (73) is satisfied for $s = 0.1$;

when t is small due possible large r_s , namely,

$$r_s = \frac{t_L r_H}{s_H}; \quad (74)$$

We next consider another region of t . We assume that the position of the resulting pole $t = s_H$ may be close to t_s , $s_H = t_s + t$, where for t there are two asymptotic limits. The first is the small t , $\frac{t}{t_s} \ll 1$, and the second for the t of the order of t_s , $\frac{t}{t_s} \sim 1$. We solve Eq. (61) by using the Green function given by Eq. (63). Due to the form of functions $\chi(r)$ the main contribution in integral of Eq. (60) comes from these $r^0 \sim r^0 \sim r_s$. Therefore, we perform the integration in Eq. (60) only over the $\chi(r)$ functions, neglecting the term proportional to r in the integrand. Using the properties of χ function, we obtain

$$\int_0^Z dr^0 \chi(r^0) \chi(r^0) = 4; \quad (75)$$

This follows from the fact that

$$\int_0^Z dr \chi(r)^2 = A \int_0^Z \frac{dq^2}{q_s^2} e^{q^2 - q_s^2} = 1;$$

When t may be small or of the order t_s , ($t = t_s + t$), i.e. $\frac{t}{t_s} \ll 1$ or $\frac{t}{t_s} \sim 1$; we obtain the following equation for resulting pole:

$$1 - s r_s \frac{r}{t_L r_H D} - \frac{4!}{t_L r_H D} \frac{1=6}{3^{2=3}} \left(\frac{1}{6}\right) - \frac{4!}{D t_L r_H} \frac{2=3}{8!^2} \frac{r_s^2}{8!^2} \left(\frac{5}{6}\right)^t = 0; \quad (76)$$

The solution of this equation for the $t = t_s + t$ with $t \ll t_s$, up to the order $\frac{t}{t_s}^2$; is:

$$t = s_H = t_s + t = \frac{2}{t_s^2 D^2} \frac{r_s^3}{3^{2=3}} \left(\frac{1}{6}\right)^3; \quad (77)$$

Fig. 7 shows the numerical solution to to Eq. (77) with $r_s = r_s^{mat}$ (see later Eq. (81)), and with $s = 0.1$. We obtain that for $s = 0.1$, $\frac{t}{t_s} = 0.3 \sim 0.8$.

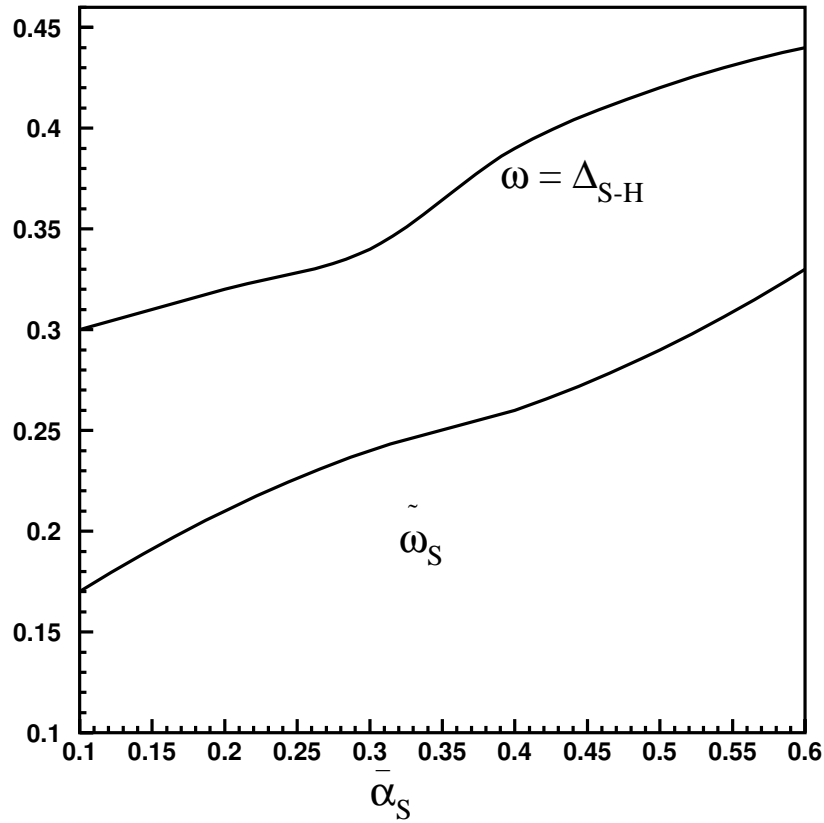


FIG. 7. Solutions for ω_{S-H} and ω_S as functions of α_S at $\alpha_s = 0.1$.

We can trust this solution only if ω is larger than ω_S , and this condition can be translated in the following inequality

$$\omega_S < \frac{2}{3} \frac{r_S}{D^2} \frac{(\frac{1}{6})^3}{3^{2=3}} : \quad (78)$$

or in the restriction on the value of ω_S

$$\omega_S < \frac{r_S^{1=3}}{D^{2=3}} \frac{2^{1=3}}{3^{2=3}} \frac{(\frac{1}{6})}{3^{2=3}} : \quad (79)$$

Remembering that Eq. (77) is valid only if $\omega_S < \omega$ we see that Eq. (78) is a solution for r_S which satisfies the inequality

$$\omega_S < \frac{r_S^{1=3}}{D^{2=3}} \frac{2^{1=3}}{3^{2=3}} \frac{(\frac{1}{6})}{3^{2=3}} : \quad (80)$$

The solution of Eq. (80) defines the region of r_S for which we can trust the approximate equation Eq. (77).

In Fig. 8, we present the solution for r_S to Eq. (80) as a function of α_S at fixed $\alpha_s = 0.1$. In Fig. 9, the same solution is plotted versus $\frac{1}{\alpha_s}$ for $D = 3$.

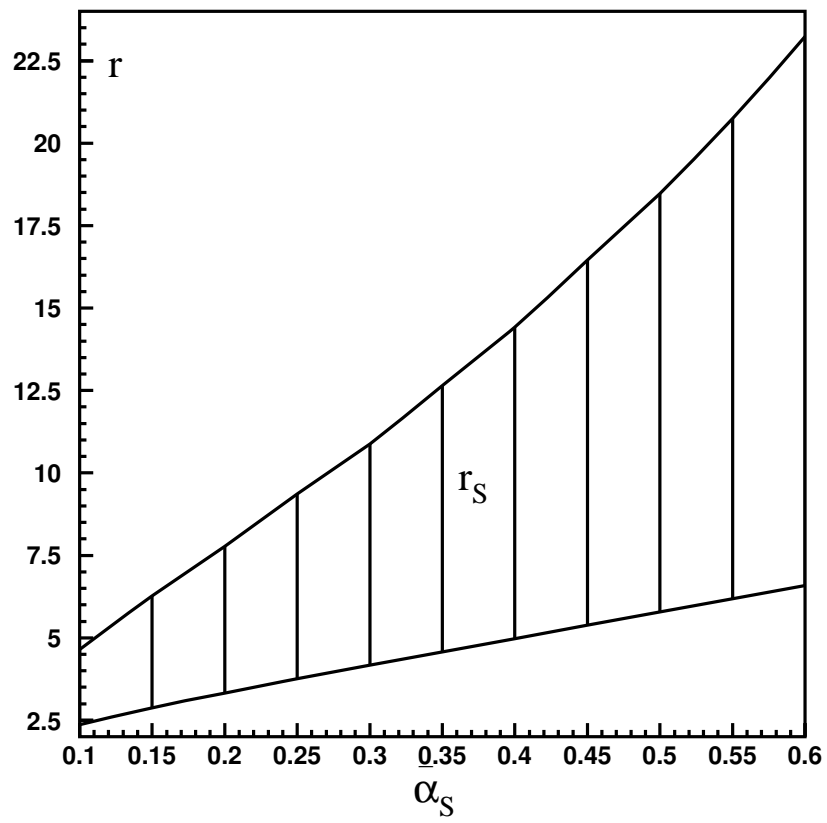


FIG .8. Permitted r_S as function of α_S at $\alpha_S = 0.1$.

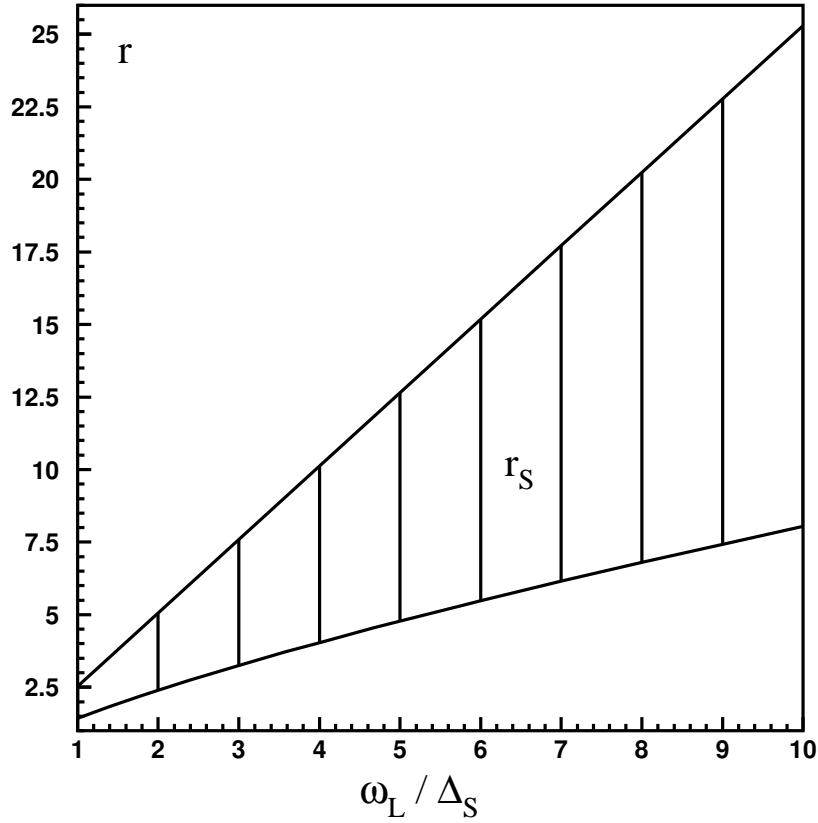


FIG .9. Permitted r_s as function of $\frac{\omega_L}{\Delta_S}$ at $D = 3$.

The matching between Eq. (77) and Eq. (71) occurs at $r_s = r_s^{mat}$ for which we have

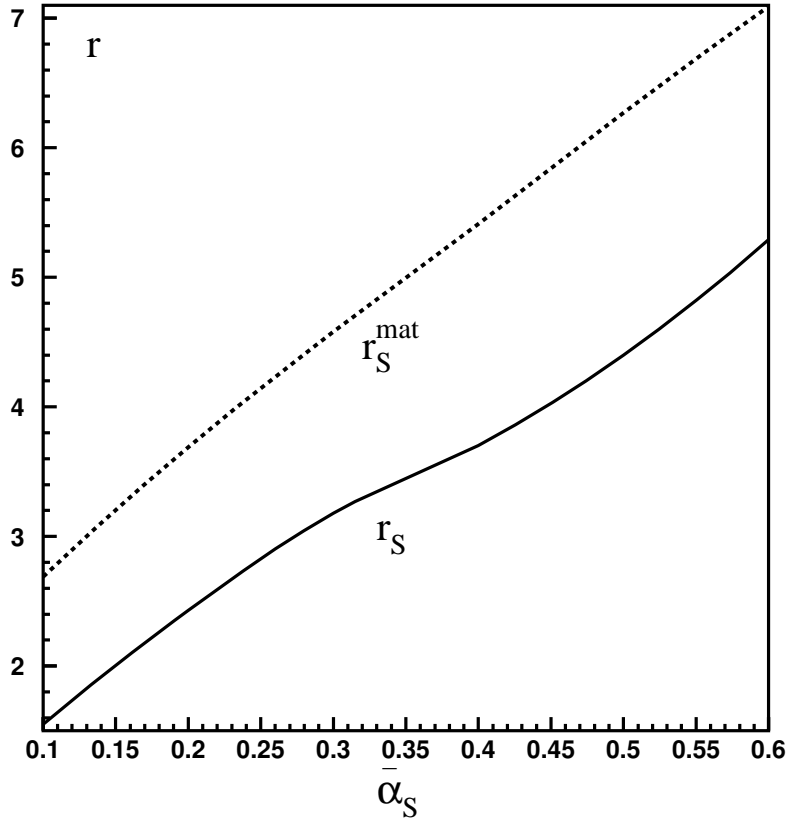
$$s_H = s + t_s + \frac{D t_s s}{96 r_s^2 (t_s + s)} = \frac{2}{t_s^2 D^2} \frac{s^3 r_s}{3^{2=3}} : \quad (81)$$

Numerical solution of this equation is presented in Fig. 10. This solution is the function of s with $s = 0.1$:

To justify the matching procedure, we have to show that, for $r_s = r_s^{mat}$ both solutions, Eq. (77) and Eq. (71), are valid. It is easy to see from Fig. 8 that r_s^{mat} calculated from Eq. (81) for any value of s , is in region where Eq. (77) has solution. From Fig. 7 we also obtain, that for given r_s the ratio $\frac{t_s}{t_s}$ is $\frac{t_s}{t_s} = 0.3 - 0.8$, and these values are satisfied the condition of Eq. (50), which defines the applicability of this solution. So, we see that solution Eq. (77) is valid for $r_s = r_s^{mat}$. Let us next consider the solution given by Eq. (71). The region of applicability of this solution is defined by Eq. (74):

$$r_s = \frac{t_L r_H}{2 s_H} \quad (82)$$

The boundary value of r_s , which is $r_s = \frac{t_L r_H}{2 s_H}$, is also presented in the Fig. 10. Considering this picture, we see, that this line lies under the r_s^{mat} defined by Eq. (81). Taking also into account, that obtained ratio $\frac{t_s}{t_s} = 0.3 - 0.8$ is satisfied the Eq. (25), we obtain, that solution Eq. (71) is also valid for the given values of r_s^{mat} :



Matching value r_S^{mat} and boundary value r_S as function of $\bar{\alpha}_S$ at $s = 0.1$.
FIG. 10.

So, finally, we have two solutions, first is Eq. (71) which is useful for r_S that lies between the lines of Fig. 10, and second is Eq. (77), which we use if r_S lies between the line for r_S^{mat} from Fig. 10 and upper bound of Fig. 8. In the following we will denote all these solutions by the s_H .

III. NLO BFKL

As have been discussed the position of the resulting singularity (pole) crucially depends on the value of β or β_L . In this section we discuss the values of β_L and D in the NLO BFKL equation [20,21]:

$$\beta = \beta_L (1 + D \beta^2); \quad (83)$$

NLO BFKL equation leads to the following values of β_L and D (see Refs. [16,21,22]):

$$\beta_L = \beta_0^2 (2.772 - 18.3 s);$$

and

$$D = s \beta_0^2 (16.828 - 322 s); \quad (84)$$

One can see that these values have a serious pathology, because for $s > 0.152$, $\beta_0^2 < 30 \text{ GeV}^2$, β_L starts to be negative and for $s > 0.05$; $\beta_0^2 < 3 \cdot 10^6 \text{ GeV}^2$ D also changes sign. Solution to this problem was

proposed by G.P. Salam [23] and M. Ciafaloni, D. Colferai and G.P. Salam [17]. They suggested a scheme to improve (resummation) the NLO BFKL kernel. Their resummation is based on the idea that the resummed NLO BFKL kernel should reproduce the NLO DGLAP one in the region of large photon virtualities. Indeed, when we start to consider the NLO terms

$$s \ln^2 \frac{s}{s_0} \quad (85)$$

and change the energy scale in the DGLAP evolution equation, namely, $s_0 = k_1^2 k_2^2$ to the energy scale $s_0 = k_1 k_2$ typical for the BFKL approach, the double logarithmic terms arise:

$$s \ln^2 \frac{k_1^2}{k_2^2} \ln^m \frac{s}{k_1 k_2} \quad (86)$$

These terms, formally subleading, nevertheless may give significant corrections to the NLO kernel. It was shown [23,17] that these terms are responsible for the difficulties with the NLO kernel. Therefore, the proposed resummation of these double logarithmic terms was done by such way, that the resummed kernel reproduces a correct DGLAP limit for $\ln^2 = 2$ and for a scale $s_0 = k_1^2$. Using this method of resummation we can avoid the difficulties of the NLO BFKL kernel. This improved kernel, of course, reproduces correctly the exact NLO BFKL kernel in the region of its applicability but it turns out to be free from inconsistency of "pure" NLO BFKL kernel. From the proposed different schemes for the improved kernel, see [23], we use scheme number four, because this scheme and also scheme number three have a reasonable behavior of second derivative of the kernel as a function $\sim s$ because the additional resummation of the terms which are important for the second derivative of the kernel there was done.

So we have:

$$\begin{aligned} & (; ; s) = \\ & s^{-1} \left(\frac{1}{1=2} + \frac{1}{=2} + \frac{1}{1=2+} + \frac{1}{=2} + \frac{1}{1=2} + \frac{1}{=2+} + \frac{1}{!=2+} + \frac{1}{s B} + \frac{1}{1=2+} + \frac{1}{=2+} + \frac{1}{!=2+} + \frac{1}{s B} \right) + \\ & \quad \frac{1}{s} \left(\frac{1}{(1=2)} + \frac{1}{(=2)^2} + \frac{1}{(1=2+)} + \frac{1}{(=2)^2} \right) + \\ & \quad \frac{1}{s} A^0 \left(\frac{1}{1=2} + \frac{1}{=2} + \frac{1}{1=2+} + \frac{1}{=2} + \frac{1}{1=2} + \frac{1}{=2+} + \frac{1}{!=2+} + \frac{1}{s B} + \frac{1}{1=2+} + \frac{1}{=2+} + \frac{1}{!=2+} + \frac{1}{s B} \right) \quad (87) \end{aligned}$$

Here

$$(; ; s) = s^{-1} \left(\frac{1}{1=2} + \frac{1}{=2} + \frac{1}{1=2+} + \frac{1}{=2} + \frac{1}{1=2} + \frac{1}{=2+} + \frac{1}{!=2+} + \frac{1}{s B} + \frac{1}{1=2+} + \frac{1}{=2+} + \frac{1}{!=2+} + \frac{1}{s B} \right) + \frac{1}{s} \left(\frac{1}{(1=2)} + \frac{1}{(=2)^2} + \frac{1}{(1=2+)} + \frac{1}{(=2)^2} \right) + \frac{1}{s} A^0 \left(\frac{1}{1=2} + \frac{1}{=2} + \frac{1}{1=2+} + \frac{1}{=2} + \frac{1}{1=2} + \frac{1}{=2+} + \frac{1}{!=2+} + \frac{1}{s B} + \frac{1}{1=2+} + \frac{1}{=2+} + \frac{1}{!=2+} + \frac{1}{s B} \right)$$

is usual BFKL kernel in the next-to-leading order, and

$$B = \frac{11}{8} - \frac{n_f}{12N_c} + \frac{n_f}{6N_c^3}; \quad (88)$$

$$A^0 = \frac{1}{2} + \frac{5n_f}{18N_c} + \frac{13n_f}{36N_c^3}; \quad (89)$$

Solving the NLO BFKL equation with improved kernel

$$! = (; ; s); \quad (90)$$

we can calculate our $NLO !_L$ and D . The results are presented in Fig. 11 and Fig. 12, where we also plotted LO $!_L$ and D . These figures show that the resummed NLO BFKL kernel gives smaller values both for $!_L$ and for D . From Fig. 11 we obtain $\dagger = 0.2$ which is rather high to describe the experimental data for soft processes. On the other hand, namely, this value of the Pomeron intercept follows from the inclusive data [29].

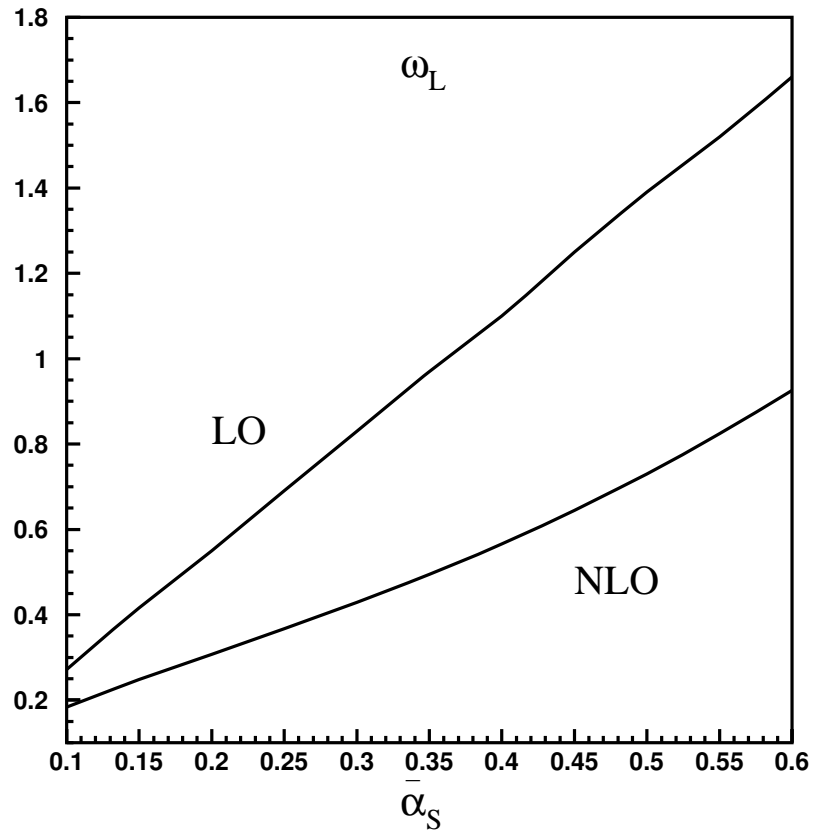


FIG . 11 .

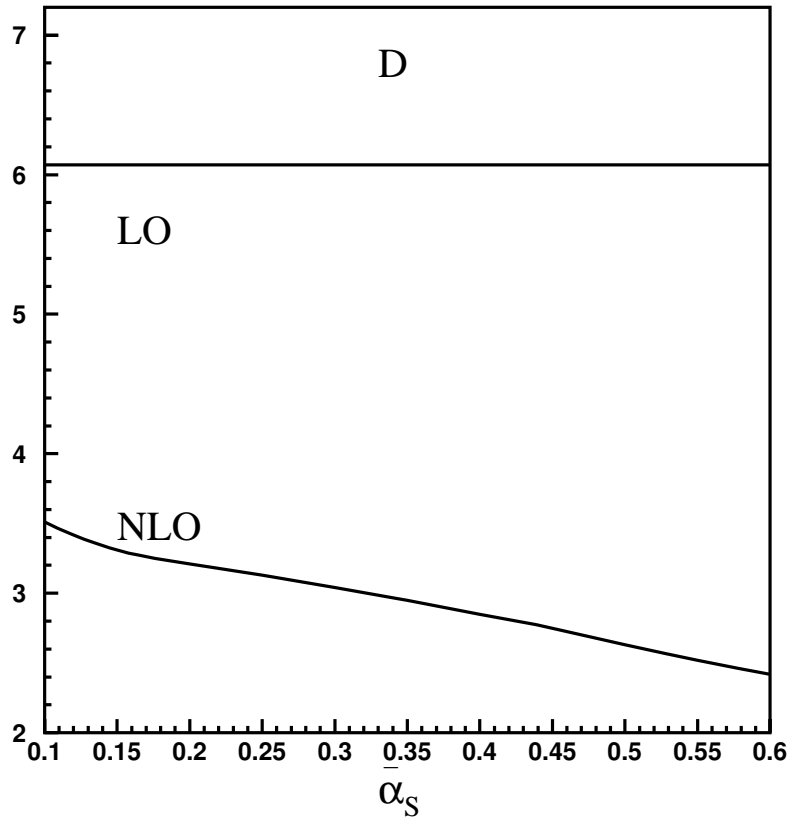


FIG . 12 .

IV . HARD AND SOFT POMERONS INTERFACE IN DIS

In this section we consider the deep inelastic processes in which we can observe the interface between soft and hard Pom erons looking at the Q^2 -dependence of the cross section (Q^2 is the photon virtuality) . The diagrams that contribute to DIS are shown in Fig. 13 .

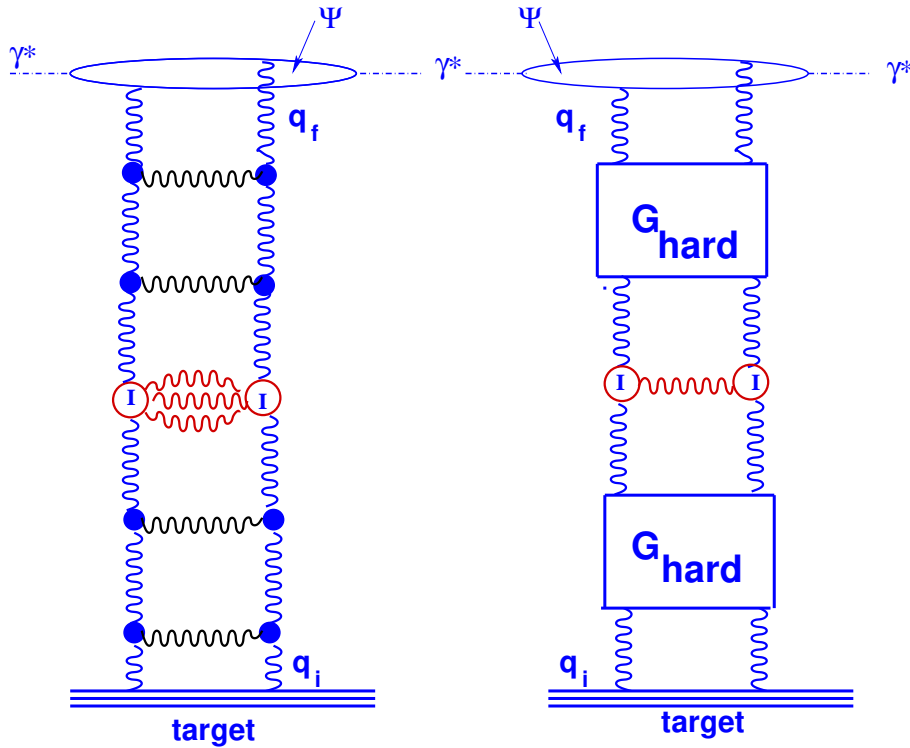


FIG. 13. Diagrams and graphic form of contributions to deep inelastic processes.

One can see that the DIS total cross section can be written in the form

$$\sigma_{\text{tot}}(p) = \int d^2 r_f d^2 r_i J(Q^2; r_f) G^{\text{DIS}}(Y; r_f; r_i) J^N(r_H; r_i); \quad (91)$$

where J and J^N are photon and nucleon impact factors which can be easily calculated in the LO of perturbative QCD (see Refs. [24] and references therein). For example,

$$J(Q^2; r_f) = \int_0^1 dz \int_0^1 dz_1 (Q^2; r_f; z)^2 \int_0^1 dz_2 e^{iq_f \cdot z} : \quad (92)$$

Introducing the Mellin integral with respect to Y

$$G^{\text{DIS}}(Y; r_f; r_i) = \frac{1}{q_f^+ q_i^-} \int_{a-1}^{a+1} \frac{d!}{2-i} \frac{s}{q_f^+ q_i^-} G_!^{\text{DIS}}(r_f; r_i); \quad (93)$$

we can sum the diagrams of Fig. 13:

$$G_!^{\text{DIS}}(r_f; r_i) = \frac{R}{1 - \int_s \frac{dr^0}{dr^0} \frac{g(!; r_f; r_i)}{dr^0} (r^0) G_H^!(r^0; r^0)}; \quad (94)$$

which can be easily understood as a simple generalization of Eq. (59) and Eq. (60).

The Green function of Eq. (94) has a quite different asymptotic than $g(!; r_f; r_i)$ due to the contribution of the denominator. This contribution stems from the zero of the denominator at $! = s_H$ which generates a Regge pole (resulting Pomeron) and our result now depends on the position of this pole and usual saddle point answer. The main question, which we want answer now is in what kinematic region in Eq. (94) the main contribution comes from the pole, which is zero of denominator of Eq. (94), and what kinematic region we have usual "hard" answer defined by $g(!; r_f; r_i)$.

First of all, we consider the region of rapidity, given by Eq. (55). Now, we have two conditions on our s_H , which should be satisfied, in order to the soft-hard pole contribution in Eq. (94) will be dominated. First of all, it is the condition of the existence of soft pole solution in denominator of Eq. (94). This condition is given by Eq. (73)–Eq. (80). Second, we have to check that this soft-hard contribution to the Green function will give larger contribution than contribution of "hard" Pomeron, given approximately by e^{t_Y} . So, it is easy to see, that both these restrictions together define the following condition for the kinematic region where the soft-hard Pomeron leads to the final answer:

$$s_H > t_Y : \quad (95)$$

We have already obtained this restriction before, see Eq. (73)–Eq. (74), and can say again, that this restriction is satisfied for the case of very small s , when $s < 0.1$ and therefore $s > t_S$, or for the case of large $\frac{r_i + r_f}{2}$, when $\frac{r_f + r_i}{2} > \frac{!_L r_H}{s_H}$. So, in both these cases asymptotic behavior of Green function will be defined by soft-hard pole. Otherwise we will stay with the answer of Eq. (54):

$$G(Y; r_f; r_i) = \frac{r}{8 Y !_L r_H D} e^{t_Y} \frac{2 - \frac{D (t_Y)^3}{(r_f + r_i)^2 = 4}}{9^{\frac{2}{3}}} \quad (96)$$

in the region of rapidity:

$$0 < Y < \frac{r_f^2}{!_L r_H} : \quad (97)$$

Another possibility for soft-hard Pomeron dominance is to have large values of rapidity. In this case the Eq. (96) is not valid anymore and we have to use equations Eq. (56)–Eq. (58). So, using Eq. 57, we can claim that for:

$$s_H > !_{SP} \quad (98)$$

we obtain the constraint on the value of rapidity for which the soft Pomeron governs the high energy asymptotic:

$$Y > \frac{!_L r_H}{D \frac{2}{s}} \quad (99)$$

Let's assume now, that we have soft-hard Pomeron regime. We want to rewrite our Green function and estimate the soft-hard Pomeron contribution. For that, first of all, we have to expand the denominator of soft-hard Pomeron, Eq. 94, with respect to $(\frac{!_L r_H}{s_H})$:

$$1 - \frac{s}{!_L r_H} = \sum_{n=0}^{\infty} \left(\frac{s}{!_L r_H} \right)^n = \sum_{n=0}^{\infty} \frac{1}{n!} \left(\frac{s}{!_L r_H} \right)^n + \dots = \frac{e^{\frac{s}{!_L r_H}}}{1} :$$

Here we take $!$ and s_H from Eq. (71). Using this expansion, we rewrite our Green function:

$$G^{DIS}(Y; r_f; r_i) = \frac{s}{q_f q_i} \sum_{a=1}^{\infty} \frac{d!}{2^a a!} \frac{s^a}{q_f q_i} \frac{g(!; r_f; r_i)}{!_{s_H}} : \quad (100)$$

Taking contour integration we obtain the answer:

$$G^{DIS}(Y; r_f; r_i) = \frac{s}{q_f q_i} \frac{s}{q_f q_i} g(! = s_H; r_f; r_i) ; \quad (101)$$

or using the Green function of Eq. (63) we have:

$$G^{DIS}(Y; r_i; r_f) = \frac{r_i}{q_f q_i} \frac{s}{!_L r_H D} \stackrel{2=3}{=} \frac{s}{q_f q_i} \stackrel{s_H}{=} : \quad (102)$$

So, concluding this consideration, we see, that we have the soft-hard, phenomenological, Pomeron contribution, determined by Eq. (102), in the following cases:

first, in the range of rapidity

$$0 < Y < \frac{r_f^2}{!_L r_H} ;$$

for the small values of s : $s < 0.1$;

second, in the range of rapidity

$$0 < Y < \frac{r_f^2}{!_L r_H} ;$$

for the large values of $\frac{r_i + r_f}{2}$:

$$\frac{r_f + r_i}{2} > \frac{!_L r_H}{s} \quad ;$$

third, for large rapidities:

$$Y \approx \frac{!_L r_H}{D} \frac{2}{s} :$$

One can see from Eq. (100) that the soft-hard transition generates a resulting Pomeron in the initial condition for the moments of the deep inelastic structure function. Therefore, in the kinematic region, where the s_H contributes, the DGLAP evolution equations only affect the Q^2 dependence of the deep inelastic structure function while the energy dependence is entirely determined by the soft Pomeron. Such a situation has been studied in details in Ref. [26]. In other kinematic regions we have a normal DGLAP evolution equation with the initial conditions which do not contain the soft-hard Pomeron contributions.

It should also be stressed that at fixed virtuality Q^2 at high energy, asymptotic behavior is determined by the exchange of the soft Pomeron independently of the value of Q^2 . However, the coupling of the soft-hard Pomeron to the photon depends on the value of the photon virtuality.

Performing estimate of our function, Eq. (102), for the case of large Q^2 , we see that the contribution of the rightmost singularity (soft-hard Pomeron) is small at large q_f . This fact makes our life more complicated and we have to remember about the infinite number of the poles that we have in Eq. (60). Indeed, these poles accumulate to zero, as will be seen later, and therefore, we face the problem of an essential singularity at zero, which possibly may give a large contribution to the Green function. So, we have to estimate the contribution of these secondary poles in $G^{DIS}(Y; r_i; r_f)$. Let's consider our variable again:

$$= \frac{4!}{D !_L r_H} \stackrel{1}{s} \frac{r_f + r_i}{2} \frac{!_L r_H}{!} g :$$

At small values of $!$ we have:

$$\frac{4}{D} \stackrel{1}{s} \frac{!_L r_H}{!} \stackrel{2}{s} : \quad (103)$$

We should calculate the contribution of the secondary poles to the Green function of Eq. (94):

$$G_{!}^{D IS}(r_f; r_i) = \frac{1}{s} \int_{dr^0} \int_{dr^{00}} \frac{G(!; r_f; r_i)}{(r^0) G_{!}^H(r^0; r^{00}) (r^{00})};$$

We rewrite this equation in the following form:

$$G_{!}^{D IS}(r_f; r_i) = \frac{r_i^2}{4 ! !_{L} r_H D} \frac{4 !}{!_{L} r_H D} \frac{1}{s} \frac{\tilde{A}i(;)}{1 - \frac{r_s}{4 r_H D !_{L} !} \frac{4 !}{D !_{L} r_H} \frac{1}{6} \tilde{A}i(; = 0)} \quad (104)$$

In the limit of small ! we can neglect 1 in the denominator of Eq. (104):

$$G_{!}^{D IS}(r_f; r_i) = \frac{r_i}{s r_s} \frac{\tilde{A}i(;)}{\tilde{A}i(; = 0)}; \quad (105)$$

The secondary pole positions are defined by the zeroes of the $\tilde{A}i(; = 0)$ function in the limit $! \rightarrow 0$. For r given by the Eq. (103) we use the steepest descent method to estimate this function. Calculated saddle points are equal to i^{2j} . They lead to contribution:

$$\tilde{A}i(; = 0) \sim \frac{r}{j} \sin\left(\frac{2}{3} j^{3/2}\right); \quad (106)$$

which together with Eq. (105) gives:

$$G_{!}^{D IS}(r_f; r_i) = \frac{r_i}{s r_s} \frac{4}{D} \frac{1}{!_{L} r_H} \frac{1}{3} \frac{\tilde{A}i(;)}{\sin\left(\frac{2}{3} j^{3/2}\right)}; \quad (107)$$

So, we obtain for the secondary pole positions the following equation (see also [13], [25]):

$$\sin\left(\frac{2}{3} \left(\frac{4}{D} \frac{1}{!_{L} r_H}\right)^{1/2} !_{L} r_H\right) = 0; \quad (108)$$

which leads to

$$!_n = \frac{2}{3} \left(\frac{4}{D} \frac{1}{!_{L} r_H}\right)^{1/2} !_{L} r_H; \quad (109)$$

Expanding \sin in Eq. (107) in the vicinity of $! = !_n$ for each n , we obtain:

$$G_{!_n}^{D IS}(r_f; r_i) = \frac{2}{3} !_{L} r_H \frac{4=3}{s r_s} \frac{r_i}{!_{L} r_H} \frac{D}{4} \frac{1}{(n)^{5=3} (!_n)} \frac{\tilde{A}i(;)}{!_n}; \quad (110)$$

Integrating over $!$ and closing contour in $!$ over the positions of the secondary poles we obtain the answer for the contribution of a separate secondary pole:

$$G_n^{D IS}(Y; r_f; r_i) = \frac{2}{3} !_{L} r_H \frac{4=3}{s r_s q_L q_f} \frac{r_i}{!_{L} r_H} \frac{D}{4} \frac{1}{(n)^{5=3}} \frac{(\tilde{A}i(;))_{!_n}}{(n)^{5=3}} e^{\frac{2}{3} \left(\frac{4}{D}\right)^{1/2} \frac{r_H !_{L} r_H}{n}} \ln \frac{s}{q_L q_f}; \quad (111)$$

The total contribution of the secondary poles is the sum over all n :

$$G^{D IS}(Y; r_f; r_i) = \frac{2}{3} !_{L} r_H \frac{4=3}{s r_s q_L q_f} \frac{r_i}{!_{L} r_H} \frac{D}{4} \frac{1}{3} \sum_n \frac{(\tilde{A}i(;))_{!_n}}{(n)^{5=3}} e^{\frac{2}{3} \left(\frac{4}{D}\right)^{1/2} \frac{r_H !_{L} r_H}{n}} \ln \frac{s}{q_L q_f}; \quad (112)$$

We can estimate the value of this sum using the steepest descent method. This estimate gives the behavior for the sum, and this contribution is smaller, than the contribution from the right-most singularity, s_H . Therefore, we can need only consider in our calculation the resulting Regge pole contribution but neglect the contribution of the secondary poles.

V . C O N C L U S I O N

This paper is a realization of old ideas to marry non-perturbative \soft" Pomeron and perturbative BFKL Pomeron [28]. The new ingredient in our approach is that the typical scale for the \soft" Pomeron is considered [3,4] to be rather large ($M_0 = 2 \text{ GeV}$ or $\xi = \ln(M_0^2 = 2^2 \cdot 4:6)$, larger than the values of transverse momenta (p_t for which we can use perturbative BFKL approach ($p_t = 1 \text{ GeV}$, $\eta = \ln(1 \text{ GeV}^2 = 2^2) = 3.2$). In other words, we assume that $r_s = \eta$.

We hoped that taking into account running QCD coupling we would be able to obtain the resulting singularity which would govern \soft" processes close to unity as it follows from the experimental observations [2]. This hope based on the fact that the BFKL Pomeron with running QCD coupling leads to singularity at angular momentum which is equal to unity. However, it turns out that even for running α_s the resulting singularity is located to the right of $!_s = !^{\text{BFKL}} \frac{r_s}{r_s}$. Using the next-to-leading order BFKL estimates for $!^{\text{BFKL}} = 0.2$ [20,21,23], we obtain $!_s = 0.139$ which is larger than the Pomeron intercept of the D-L phenomenological Pomeron [2]. However, the estimates of the Pomeron intercept from the single inclusive production lead to higher value of the Pomeron intercept [29] which are in a better agreement with our predictions.

The main result of this paper is concentrated in Eq. (71) and Eq. (77) which give the position of the resulting singularity for different ranges of α_s and non-perturbative input α_s . We discussed also the interplay between the BFKL Pomeron and the resulting Pomeron in deep inelastic process which gives us a possibility to measure the hard BFKL Pomeron at large virtualities of photon and to investigate the matching between \soft" and \hard" pomeron for small values of the photon virtualities. To our great surprise our result shows (see Eq. (102)) that even at large photon virtualities the contribution of the resulting singularity is dominant at high energy (low x). In other words we cannot consider DIS at low x as a typical hard process where we can safely use perturbative QCD. The admixture of non-perturbative interaction is so essential that it changes the effective Pomeron intercept.

It is interesting to compare our model with the model introduced in Ref. [18], where two Pomeron model was also introduced. We have no ideological disaccords with this model and we differ from it in a way how a transition from soft to hard Pomerons is occurred and in origin of soft Pomeron. We assumed that the existence of the soft Pomeron is related to typical non-perturbative phenomena as QCD instantons and/or the scale anomaly in QCD while in Ref. [18] M. Ciafaloni, M. Tauti and A. H. Mueller study a possibility that the non-perturbative Pomeron would be generated by the behavior of the QCD coupling at low values of transverse momenta. Our \soft" Pomeron has normal Gribov duality in impact parameters which we match with duality in transverse momenta which is typical for the BFKL Pomeron. The freezing of the QCD coupling leads to a new picture which was suggested in Ref. [27] and which is certainly an alternative approach to ours.

We would like to stress that in this paper we consider only the interface of two Pomerons: the soft Pomeron and the BFKL Pomeron. The reality could be much richer and could follow to another scenario of matching the long distance interaction with the short distance QCD physics. As was pointed out in Ref. [30], the soft Pomeron could be suppressed if it is build from QCD instantons, [4], in the high parton density environment. In other words, if the interface between long and short distances interaction passes the stage of high parton density QCD the soft Pomeron does not contribute to the high energy asymptotic behavior of the scattering amplitude.

We consider the observation that the non-perturbative correction could be essential for so called \hard" process at low x and large scale of hardness (like DIS at low x) as the main result of this paper.

Acknowledgments:

We wish to thank Jochen Bartels, Errol Gotsman and Uri Marmor for very fruitful discussions on the subject.

We would like to thank the DESY Theory Group and the BNL Nuclear Theory Group for their hospitality and creative atmosphere during several stages of this work.

E.L. is indebted to the Alexander-von-Humboldt Foundation for the award that gave him a possibility to work on high energy physics during the last year.

This research was supported in part by the GIF grant # I-620-22.14/1999, and by the Israel Science Foundation, founded by the Israeli Academy of Science and Humanities.

Special thanks go to the Dima Kharzeev and Yuri V. Kovchegov who took part in the first part of the research and whose discussions and support were very helpful.

-
- [1] E.A. Kuraev, L.N. Lipatov and V.S. Fadin, *Sov. Phys. JETP* 45 (1977) 199;
 Ia.Ja. Balitsky and L.N. Lipatov, *Sov. J. Nucl. Phys.* 28 (1978) 822;
 L.N. Lipatov, *Sov. Phys. JETP* 63 (1986) 904.
- [2] A. Donnachie and P.V. Landsho, *Nucl. Phys. B* 244 (1984) 322; *Nucl. Phys. B* 267 (1986) 690; *Phys. Lett. B* 296 (1992) 227; *Z. Phys. C* 61 (1994) 139.
- [3] D. Kharzeev and E. Levin, *Nucl. Phys. B* 578 (2000) 351, hep-ph/9912216.
- [4] D. Kharzeev, Yu. Kovchegov and E. Levin, *Nucl. Phys. A* 690 (2001) 621, hep-ph/0007182.
- [5] E.V. Shuryak, hep-ph/0101269; Maciek A. Nowak, E.V. Shuryak, and I. Zahed, *Phys. Rev. D* 64 (2001) 034008; hep-ph/0012232 and references therein.
- [6] A.B. Kaidalov and Yu.A. Simonov, *Phys. Lett. B* 477 (2000) 163;
- [7] R.A. Janik and R. Peschanski, *Nucl. Phys. B* 586 (2000) 163; *B* 565 (2000) 193, hep-th/9907177;
 R.A. Janik, *Phys. Lett. B* 500 (2001) 118, hep-th/0010069;
 K. Tuchin, *Phys. Lett. B* 497 (2001), hep-ph/0007311.
- [8] M. Genovese, N.N. Nikolaev and B.G. Zakharov, *JETP* 81 (1995) 625;
 B.Z. Kopeliovich, I.K. Potashnikova, B. Povh and E. Predazzi, *Phys. Rev. Lett.* 85 (2000) 507.
- [9] B.C. Bower, S.D. Mathur and Chung-I Tan, *Nucl. Phys. B* 587 (2000) 249, hep-ph/0003153.
- [10] L.V. Gribov, E.M. Levin, and M.G. Ryskin, *Phys. Rep.* 100, 1 (1983).
- [11] A.H. Mueller, J.-W. Qiu, *Nucl. Phys. B* 268, 427 (1986);
 L.M. McLerran and R. Venugopalan, *Phys. Rev. D* 49, 2233 (1994); *D* 49, 3352 (1994); *D* 50, 2225 (1994).
- [12] J.C. Collins and J. Kwiecinski, *Nucl. Phys. B* 316 (1989) 307.
- [13] E. Levin, *Nucl. Phys. B* 453 (1995) 303; "ORSAY lectures on low x deep inelastic scattering" *LPTHE, Orsay* 91/02.
- [14] Yu.V. Kovchegov and A.H. Mueller, *Phys. Lett. B* 439 (1998) 428.
- [15] N. Armesto, J. Bartels and M.A. Braun, *Phys. Lett. B* 442 (1998) 459.
- [16] E. Levin, *Nucl. Phys. B* 445 (1999) 481, hep-ph/9806228.
- [17] M. Ciafaloni, D. Colferai and G.P. Salam, *JHEP* 9910 (1999) 017 and 0007 (2000) 054.
- [18] M. Ciafaloni, M. Taati and A.H. Mueller, *Nucl. Phys. B* 616 (2001) 349, hep-ph/0107009.
- [19] "Regge Theory of Low p_T Hadronic Interaction", editor L. Caneschi, North-Holland, 1989.
- [20] V.S. Fadin and L.N. Lipatov, *Phys. Lett. B* 429 (1998) 127 and references therein.
- [21] G. Camici and M. Ciafaloni, *Phys. Lett. B* 412 (1997) 396, *B* 430 (1998) 349.
- [22] D.A. Ross, *Phys. Lett. B* 431 (1998) 161.
- [23] G.P. Salam, *JHEP* 9807 (1998) 019.
- [24] J. Bartels, A. De Roeck, C. Ewerz and H. Lotter, "The total cross section and the BFKL Pomeron at 500 GeV e^+e^- linear collider", hep-ph/971050;
 S.J. Brodsky, F. Hautmann and D.E. Soper, *Phys. Rev. D* 56 (1997) 6957.
- [25] L.P. Aharony, O.V. Kancheli and J.K. Koch, *Phys. Lett. B* 391 (1997) 157; *Nucl. Phys. B* 518 (1998) 275.
- [26] C. Lopez and F.J.Y. Durain, *Phys. Rev. Lett.* 44 (1980) 1118;
 C. Lopez and F.J.Y. Durain, *Nucl. Phys. B* 171 (1980) 231;
 A. Donnachie and P.V. Landsho, *Phys. Lett. B* 437 (1981) 408;
 R.K. Ellis, Z. Kunszt and E. Levin *Nucl. Phys. B* 420 (1991) 517.
- [27] M. Ciafaloni, D. Colferai, G.P. Salam and A.M. Stasto, *Phys. Lett. B* 541 (2002) 314, hep-ph/0204287.
- [28] E. Levin and C.I. Tan, "Heterotic pomeron: A Unified treatment of high-energy hadronic collisions in QCD", hep-ph/9302308.
- [29] A.K. Likhoded, N.V. Mokhov and O.P. Yushchenko, "Bare Pomeron In Inclusive Processes", FERMILAB-FN-0504, Jan. 1989; P.V. Chliapnikov, A.K. Likhoded and V.A. Uvarov, *Phys. Lett. B* 215 (1988) 417;
 A.B. Kaidalov and K.A. Ter-Martirosian, *Sov. J. Nucl. Phys.* 39 (1984) 979 A.B. Kaidalov, *Phys. Lett. B* 116 (1982) 459.
- [30] D.E. Kharzeev, Y.V. Kovchegov and E. Levin, *Nucl. Phys. A* 699 (2002) 745, hep-ph/0106248.